PNAS
www.pnas.org

Supplementary Information for

Large-scale ratcheting in a bacterial DEAH/RHA-type RNA helicase that modulates antibiotics susceptibility

Lena M. Grass, Jan Wollenhaupt, Tatjana Barthel, Iwan Parfentev, Henning Urlaub, Bernhard Loll, Eberhard Klauck, Haike Antelmann, Markus C. Wahl

Correspondence to: Markus C. Wahl
Email: markus.wahl@fu-berlin.de

This PDF file includes:

Other supplementary materials for this manuscript include the following:

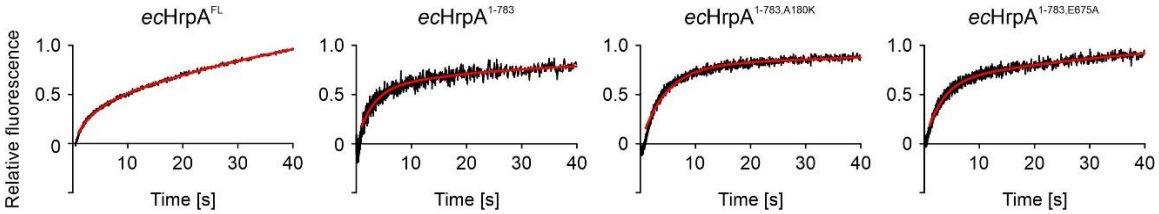

Fig. S1. Fitting of stopped-flow/fluorescence data. The data were fitted to a double exponential equation (fraction unwound = $A_{fast} \cdot (1-\exp(-k_{fast}t)) + A_{slow} \cdot (1-\exp(-k_{slow}t))$; A, total unwinding amplitude; k, unwinding rate constants [s^{-1}]; t, time [s]), as described (1, 2). The first second of data acquisition was excluded from curve fitting to account for the initial mixing periods. Amplitude-weighted unwinding rate constants were calculated as $k_{unw} = \sum(A_i k_i^2)/\sum(k_i A_i)$. Curve fitting yielded data shown in Fig. 2D and Fig. 2H and listed in SI Appendix, Table S2.

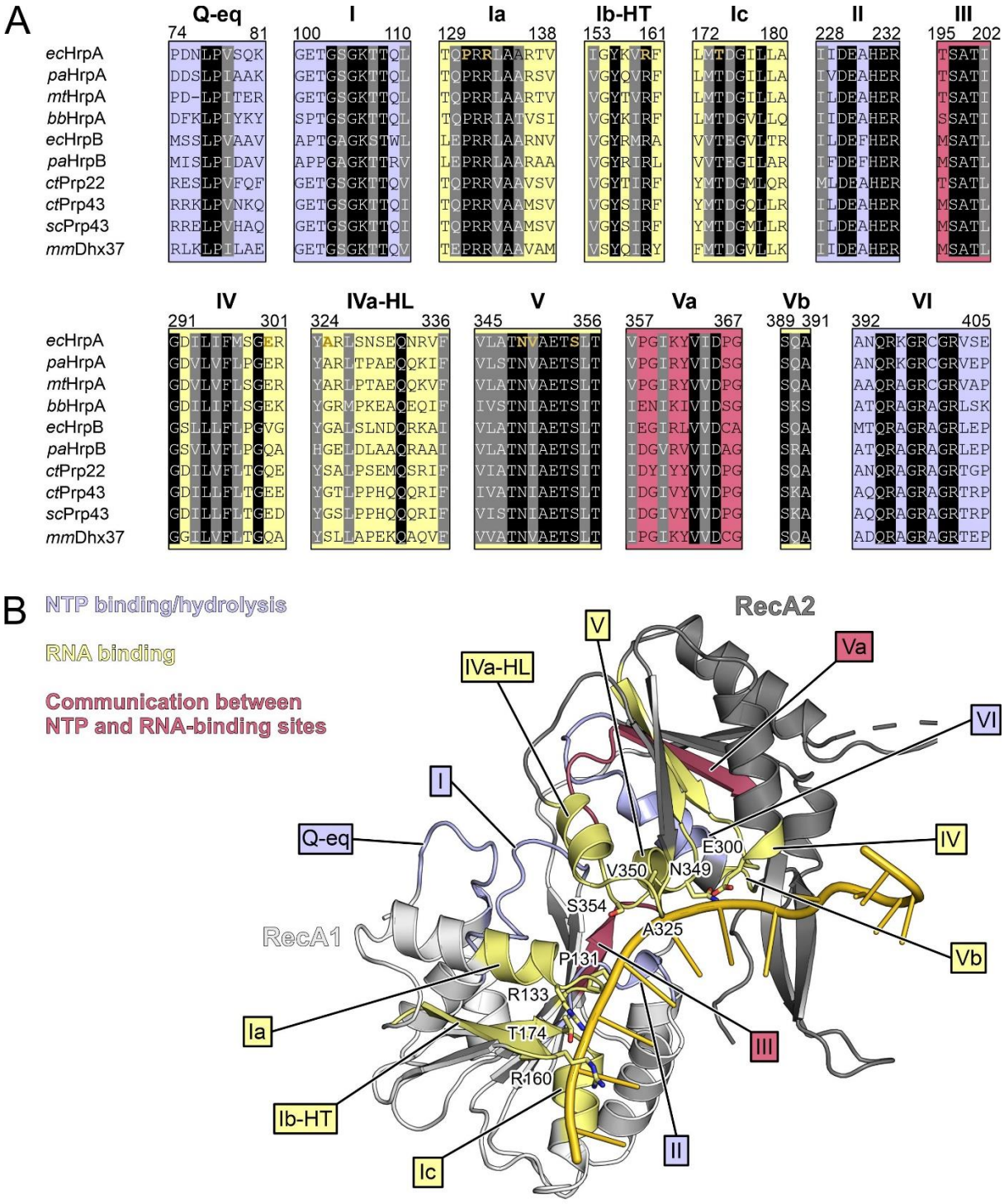

Fig. S2. Conserved helicase motifs. (*A*) Multiple sequence alignment of helicase core motifs (indicated above the alignment) in bacterial and eukaryotic DEAH/RHA proteins. Q-eq, equivalent of the Q motif; HT, hook-turn; HL, hook-loop; *ec*, *E. coli*; *pa*, *Pseudomonas aeruginosa*; *mt*, *Mycobacterium tuberculosis*; *bb*, *Borrelia burgdorferi*; *ct*, *Chaetomium thermophilum*; *sc*, *Saccharomyces cerevisiae*; *mm*, *Mus musculus*. Invariant residues, black background; highly conserved residues, gray background; RNA-interacting residues of *ec*HrpA$^{1\text{-}783}$, gold. Residue numbering above the alignment refers to *ec*HrpA. The background colors of the motif boxes

indicate the involvement of the respective motif in NTP binding/hydrolysis (blue), communication between NTP and RNA-binding sites (red) or RNA binding (yellow). (*B*) Cartoon plot of the RecA-like domains and bound RNA of the *ec*HrpA$^{1\text{-}783}$-U_{15} crystal structure. Residues shown as sticks and labeled, RNA-interacting residues of *ec*HrpA$^{1\text{-}783}$ (highlighted in gold in the multiple sequence alignment).

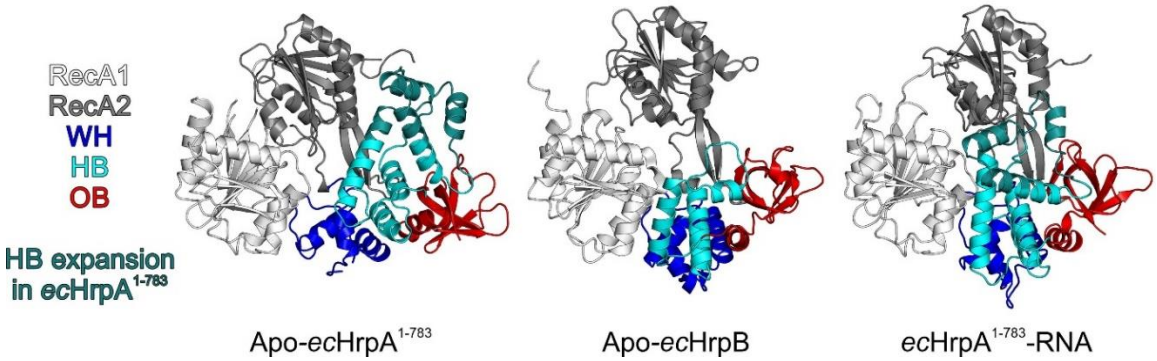

Fig. S3. Comparison of the conformations of the DEAH/RHA-like helicase cassettes in apo-ecHrpA$^{1-783}$ (left), apo-ecHrpB (middle) and RNA-bound ecHrpA$^{1-783}$ (right). The apo-ecHrpB conformation resembles that of RNA-bound ecHrpA$^{1-783}$. Expansion elements of the ecHrpA$^{1-783}$ HB domain, teal.

Table S1. Oligonucleotides employed[(a)]

Oligonucleotide	Source
Primers for construction of *hrpA::kan* mutant	
HrpA-up: 5'-TAATACCTTGCTCATGGTGTTTCC-3'	Microsynth Seqlab
HrpA-down: 5'-GTGAGATAATAGTGAGAAGCGG-3'	
ctrl-K1: 5'-CAGTCATAGCCGAATAGCCT-3'	
ctrl-K2: 5'-CGGTGCCCTGAATGAACTGC-3'	
Primers for cloning into pBAD LIC (8A) vector	
pBAD_fw: 5'-AGGATCCCTTGGCTGTTTTG-3'	Microsynth Seqlab
pBAD_rv: 5'-GGGATATCTATATCTCCTTCTTAAAGTTAAAC-3'	
ecHrpA_pBAD_fw: 5'-TGATTATAAAGACGATGATGACAAGATGACAGAACAACAAAAATTGACCTTTACG-3'	
ecHrpA_pBAD_rv: 5'-TCCGCCAAAACAGCCAAGGGATCCTTTAACCGCTAATCTGCTCCATCG-3'	
tag_fw: 5'-TTTAAGAAGGAGATATAGATATCCCATGAACCACCATCACCACCACCATGCAGGAAAAGC-3'	
tag_rv: 5'-AGGTCAATTTTTGTTGTTCTGTCATCTTGTCATCATCGTCTTTATAATCAATATCATGGTCCTTA TAATCG-3'	
Primers for cloning into pETM-11 vector	
ecHrpA_fw: 5'-TCTTTATTTTCAGGGCGCCATGGCGATGACAGAACAACAAAAATTGACCTTTAC-3'	Eurofins Genomics
ecHrpA_rv: 5'-TGTCGACGGAGCTCGAATTCGGTTAACCGCTAATCTGCTCCATCG-3'	
ecHrpA(1-783)_fw: 5'-GCGGCCGCACTCG-3'	
ecHrpA(1-783)_rv: 5'-TTATGATTTGTGTTCCAGCTCTTCTACTTCC-3'	
ecHrpA(784-1300)_fw: 5'-CGTCGCCGCGATATTCTG-3'	
ecHrpA(784-1300)_rv: 5'-GCCCTGAAAATAAAGATTCTCAGTAGTGG-3'	
ecHrpA(909-1300)_fw: 5'-TCGTTGCCGAAACCGGTA-3'	
ecHrpA(909-1300)_rv: 5'-GCCCTGAAAATAAAGATTCTCAGTAGTGG-3'	
Primers for introducing point mutations *via* inverse PCR	
ecHrpA_K106A_fw: 5'-CAACGACTCAGTTACCGAAAATCTGTATGG-3'	Eurofins Genomics
ecHrpA_K106A_rv: 5'-CACCAGAACCCGTTTCCCCGG-3'	
ecHrpA(1-783)_D305A_fw: 5'-CCGATGCGCTGAACAAGCTG-3'	
ecHrpA(1-783)_D305A_rv: 5'-CGGTAGCGCGGATTTCCCG-3'	
ecHrpA(1-783)_E675A_fw: 5'-CAACCAGCCGCCTGTGGGG-3'	
ecHrpA(1-783)_E675A_rv: 5'-CTACCAGTTCCGCCACCATTACC-3'	
ecHrpA(1-783)_A180K_fw: 5'-AGAGATCCAGCAAGACCGCC-3'	
ecHrpA(1-783)_A180K_rv: 5'-TTCAGCAGGATACCGTCGGTC-3'	
ecHrpA(1-783)_FP_fw: 5'-GCCGGTTCTGGTTTATTCAAAAAA-3'	
ecHrpA(1-783)_FP_rv: 5'-GGCGATGGAGAAACGCGCGTTAC-3'	
Oligonucleotide for RNA binding assays	
FAM-RNASS15: [5-FAM]-5'-GCUGCCAGACCAAAU-3'	IBA
FAM-RNABlunt: 5'-**GCUGCCAGACCAAAU**-3'-[5-FAM] 5'-**AUUUGGUCUGGCAGC**-3'	
FAM-RNA3'ovh: 5'-**GACCAGCACGCG**-3' 5'-**CGCGUGCUGGUC**UAAACCAGACCGUCG-3'-[5-FAM]	

FAM-RNA5'ovh: 5'-**GCGCACGACCAG**-3' [5-FAM]-5'-GCUGCCAGACCAAAU**CUGGUCGUGCGC**-3'	
FAM-RNAFork: 5'-**GCGCACGACCAG**GAAAUUUAAUUAUAA-3'-[5-FAM] 5'-GCUGCCAGACCAAAU**CUGGUCGUGCGC**-3'	
FAM-DNASS16: [5-FAM]-5'-TATAAACCAGACCGTC-3'	
Oligonucleotides for unwinding assays	
RNA3'ovh: [Atto540Q]-5'-GGCCGCGAGCCGGAAAUUUAAUUAUAAACCAGACCGUCUCCUC-3' 5'-**CGGCUCGCGGCC**-3'-[Alexa488]	IBA
RNA5'ovh: 5'-CUCCUCUGCCAGACCAAAUAUUAAUUUAAAG**GCCGAGCGCCGG**-3'-[Atto540Q] [Alexa488]-5'-**CCGGCGCUCGGC**-3'	
DNA_3'ovh: [Atto540Q]-5'-**GGCCGCGAGCCG**GAAATTTAATTATAAACCAGACCGTCTCCTC-3' 5'-**CGGCTCGCGGCC**-3'-[Alexa488]	
Oligonucleotides for crystallization and ATPase assay	
RNA_U_15: 5'-UUUUUUUUUUUUUUU-3'	IBA
DNA_19nts: 5'-GCGTCCCAGTCCGGCATCT-3'	Eurofins Genomics

[a] Complementary regions in bold

Table S2. Helicase parameters quantified based on data shown in Fig. 2D and Fig. 2H

***ec*HrpA variant**	***ec*HrpA^{FL}**	***ec*HrpA$^{1-783}$**	***ec*HrpA$^{1-783,A180K}$**	***ec*HrpA$^{1-783,E675A}$**
k_{fast} [s^{-1}]	0.32	0.36	0.26	0.33
k_{slow} [s^{-1}]	0.02	0.04	0.02	0.02
A_{fast}	0.31	0.53	0.72	0.62
A_{slow}	1.21	0.31	0.28	0.52
R^2	0.9417	0.7039	0.9141	0.9503
Absolute sum of squares	20.29	68.80	11.44	7.72
k_{unw} [s^{-1}]	0.26	0.34	0.25	0.31
Fold-FL (k_{unw})	1.00	1.30	0.96	1.18

Table S3. Crystallographic data[a]

Dataset	$HrpA^{1-783,\ SeMet}$	$HrpA^{1-783,D305A}$	$HrpA^{1-783,SeMet}$	$HrpA^{1-783}$-U_{15}
PDB entry	6ZWX	7AKP	-	6ZWW
Data collection				
Wavelength [Å]	0.9184	0.9184	0.980	0.9184
Temperature [K]	100	100	100	100
Space group	$P2_1$	$P2_1$	$P2_1$	C2
Unit cell parameters				
a, b, c [Å]	40.1, 116.5, 92.6	39.9, 114.9, 94.6	40.0, 117.0, 94.5	220.8, 126.2, 179.2
α, β, γ [°]	90.0, 98.6, 90.0	90.0, 102.0, 90.0	90.0, 99.6, 90.0	90.0, 110.8, 90.0
Resolution [Å]	50.00 - 2.70 (2.85 - 2.70)	50.00 - 2.59 (2.75 - 2.59)	50.00 - 3.00 (3.18 - 3.00)	50.00 - 3.19 (3.34 - 3.15)
Reflections				
Unique	23,139 (3,427)	25,697 (4,048)	50,272 (3,581)	78,441 (12,390)
Completeness [%]	99.9 (99.4)	99.2 (97.0)	99.6 (95.3)	99.0 (97.5)
Multiplicity	12.9 (8.7)	6.9 (6.8)	28.4 (27.8)	5.0 (4.8)
Data quality				
Intensity [I/σ(I)]	12.9 (0.8)	7.3 (0.8)	9.3 (0.8)	8.9 (0.5)
R_{meas} [%][b]	12.1 (219.3)	30.1 (266.6)	45.6 (380.9)	14.6 (320.5)
$CC_{1/2}$[c]	99.3 (41.1)	98.7 (33.3)	99.5 (35.6)	99.8 (22.4)
Wilson B value [$Å^2$]	87.3	56.6	89.8	105.8
Phasing				
Number of Se atoms			16	
Figure of merit			0.558	
Refinement				
Resolution [Å]	50.00 - 2.70 (2.82 - 2.70)	50.00 - 2.60 (2.70 - 2.59)		49.40 - 3.16 (3.27 - 3.16)
Reflections				
Number	23,311	25,695		78,400
Test set [%]	5.0	5.0		2.7
R_{work} [%]	22.4 (36.9)	21.1 (36.9)		22.3 (52.9)
R_{free} [%]	27.6 (39.5)	31.2 (32.4)		26.3 (51.2)
Asymmetric unit				
Non-hydrogen atoms	5,912	5,800		24,593
Protein residues	736	723		2,959
RNA nucleotides	-	-		44
Water molecules	11	-		-
Mean temperature factors [$Å^2$]				
All atoms	102.3	70.5		144.8
Protein	102.3	70.5		127.7
RNA	-	-		145.1
Water	92.1	-		-
RMSD[d] from target geometry				
Bond lengths [Å]	0.004	0.003		0.004
Bond angles [°]	0.617	0.615		0.781
Validation				
Ramachandran plot[e]				
Favored [%]	96.6	96.2		96.3
Disallowed [%]	0.3	0.7		0.2
Ramachandran Z-score[e]				
All	-1.79	-3.23		-1.78
Helices	-1.59	-2.59		-1.42
Sheets	-0.95	-1.34		-0.31
Loops	-0.51	-1.67		-1.04
MOLPROBITY scores[f]				
Clashscore[g]	6.55	9.40		11.69
Score	1.98	2.29		1.83

[a] Data for the highest resolution shells in parentheses

[b] $R_{meas}(I) = \sum_h [N/(N-1)]^{1/2} \sum_i \left| I_{ih} - \langle I_h \rangle \right| / \sum_h \sum_i I_{ih}$, in which $\langle I_h \rangle$ is the mean intensity of symmetry-equivalent reflections h, I_{ih} is the intensity of a particular observation of h and N is the number of redundant observations of reflection h (3)

[c] $CC_{1/2} = (\sigma^2_\tau) / (\sigma^2_\tau + \sigma^2_\varepsilon)$, in which σ^2_τ is the variance of τ, σ^2_ε is the variance of $\varepsilon_{A,B}$, τ is the difference between true values of intensities and their average, $\varepsilon_{A,B}$ are the random errors in merged intensities of half-sized subsets (4)

[d] RMSD, root mean square deviation

[e] Calculated with PHENIX (5)

[f] Calculated with MOLPROBITY (6)

[g] Clashscore is the number of serious steric overlaps (> 0.4) per 1,000 atoms (6)

Table S4. Cross-links between residues on domains that undergo conformational rearrangements[(a)]

Cross-linked residues	Log2 ratio apo/RNA	Cα-Cα distance apo-*ec*HrpA$^{1-783}$ [Å]	Cα-Cα distance *ec*HrpA$^{1-783}$-U$_{15}$ [Å]
K106-K361	0.58	22.0	24.9
K312-K570	1.02	18.4	45.8
K485-K721	0.50	30.9	33.3
K312-K537	-0.89	32.2	19.1
K312-K544	-1.06	30.8	29.6
K312-K662	-0.76	48.8	33.4

[a] Green entries, more abundant in apo-*ec*HrpA$^{1-783}$; orange entries, more abundant in *ec*HrpA$^{1-783}$-U$_{15}$

Movie S1 (separate file). Movie S1 shows a morph between apo and RNA-bound conformations of *ec*HrpA$^{1-783}$ viewed in two orientations. For this and the following movie, coordinates were morphed with PyMOL (Schrödinger Inc.; https://pymol.org/2). The movies were compiled with Shotcut (https://www.shotcut.org).

Movie S2 (separate file). Movie S2 shows comparative morphs between apo and RNA-bound conformations in *ec*HrpA$^{1-783}$ and *C. thermophilum* Prp22 (PDB IDs 6I3O and 6I3P).

Dataset S1 (separate file). Results from quantitative cross-linking mass spectrometry using isotopic labels. Sheet 'All' contains all identified and quantified unique cross-linked residues, sheet 'Rearranged domains' contains cross-links between residues on domains that undergo conformational rearrangements (see also SI Appendix, Table S4).

SI References

1. A. R. Ozes, K. Feoktistova, B. C. Avanzino, E. P. Baldwin, C. S. Fraser, Real-time fluorescence assays to monitor duplex unwinding and ATPase activities of helicases. *Nat. Protoc.* **9**, 1645-1661 (2014).
2. J. J. Roske, S. Liu, B. Loll, U. Neu, M. C. Wahl, A skipping rope translocation mechanism in a widespread family of DNA repair helicases. *Nucleic Acids Res.* **49**, 504-518 (2021).
3. K. Diederichs, P. A. Karplus, Improved R-factors for diffraction data analysis in macromolecular crystallography. *Nat. Struct. Biol.* **4**, 269-275 (1997).
4. P. A. Karplus, K. Diederichs, Linking crystallographic model and data quality. *Science* **336**, 1030-1033 (2012).
5. P. D. Adams *et al.*, PHENIX: a comprehensive Python-based system for macromolecular structure solution. *Acta Crystallogr. D Biol. Crystallogr.* **66**, 213-221 (2010).
6. C. J. Williams *et al.*, MolProbity: More and better reference data for improved all-atom structure validation. *Protein Sci.* **27**, 293-315 (2018).